ELSEVIER

Thermochimica Acta 310 (1998) 133–140

thermochimica acta

Thermal analytical study of steels at high temperature including the range of melting[1]

A. Lindemann, J. Al-Karawi, J. Schmidt*

Otto-von-Guericke-Universität Magdeburg, Institut für Strömungstechnik und Thermodynamik, Abt. Thermodynamik, Universitätsplatz 2, D-39106 Magdeburg, Germany

Received 20 May 1997; received in revised form 12 June 1997; accepted 16 June 1997

Abstract

Measurements with a plate transducer, up to 1600°C, are investigated in the current paper. The calibration of the transducer, comparative measurements concerning the accuracy of specific heat capacity determination, the modelling for the high-temperature range and results for three steels are presented. The results are used to develop the database *dbs* for thermal simulation computations. © 1998 Elsevier Science B.V.

Keywords: Database; Differential scanning calorimetry; Heat capacity; Phase change enthalpy; Steels

1. Introduction

Ensuring availability of secured thermal properties of metallic substances has great importance for the thermal process simulation, which is of growing interest in many fields of metallurgy, metal forming, manufacturing and joining techniques.

The numeric analysis often considerably reduces the experimental expenditure during the technology processing. For example, in the case of welding, the knowledge of the temperature field and of the joint geometry is the basis for process optimization. From these, the quality of the joint and the crystalline structure in the heat-influence zone can be derived [1,2]. For low-alloy steels, the cooling time between 800° and 500°C ($t_{8/5}$-time) decisively influences the structural shape. Computations with the developed programme system *TENAS* [3] showed that the use of reliable material properties is an essential precondition for precise simulation calculations. In particular, the melting enthalpy $\Delta_p h$ and the melting temperature T_p have an essential influence on the $t_{8/5}$-time besides the specific heat capacity. For this reason, a database for steels is built-up, which contains the heat capacity dependent on the temperature, the phase change enthalpies and their assigned temperatures. This is planned both, as an extra module for the mentioned programme system *TENAS* and as a stand-alone information programme.

However, there are great gaps in the availability of thermophysical properties of steels, in particular >1000°C. In connection with simulations, special materials and, above all, newly developed steels require experimental investigations in order to obtain the characteristic thermophysical properties.

*Corresponding author. Tel.: 00 49 391/67-18575, -18576; fax: 00 49 391/67-12762;
e-mail: juergen.schmidt@mb.uni-magdeburg.de

[1]Presented at the Twelfth Ulm-Freiberg Conference, Freiberg, Germany, 19–21 March 1997

PII S0040-6031(97)00390-0

2. Experimental

Measurements were carried out with the thermal analysis system SETARAM TGA 92 and a DSC plate transducer with platinum/rhodium thermocouples (type B). The graphite resistor furnace is usable up to 1600°C. The calibration of the transducer and comparative measurements are presented. All runs were done at the heating rate of 3 K/min. The use of platinum crucibles is especially useful for heat-capacity measurements. However, because they are not suitable for steels, nor could long-time stability be achieved with platinum-coated alumina crucibles, a measuring variant is described which makes use of an Al_2O_3 sample crucible and a platinum reference crucible. The model of heat-capacity determination and preliminary measurements for three different steels are presented in this paper.

2.1. Preliminary investigations

The use of a DSC plate transducer for the determination of the specific heat capacity did not ensure precise results, particularly in the high-temperature range. Therefore, after evaluation of literature [4,5], preliminary investigations were carried out with the aim of an improvement in sensitivity and reproducibility. Helium and argon were used as carrier gases. Helium has a considerably better thermal conductivity ($\lambda_{He} \approx 9\lambda_{Ar}$ at 1000°C), which reduces the thermal resistance between the crucibles and the transducer.

Correspondingly, the series of measurements using helium showed a better reproducibility in spite of a lower DSC signal (Fig. 1). The use of crucibles with lids improved the reproducibility too. The specified heat-transfer conditions are managed in this manner for the sample cylinder. The comparison between Al_2O_3 and platinum crucibles yielded better results using platinum crucibles. However, these crucibles cannot be used for steels in the range of high temperatures. For this reason, Al_2O_3 crucibles were coated with platinum (vacuum evaporation and sputtering). But the achieved coatings showed no long-time stability. Every heating process caused a change of the emissivity and, therefore, a change of the heat-transfer conditions. Reproducible measurements could not be achieved in this manner. The emissivity ε was controlled using the infrared thermography

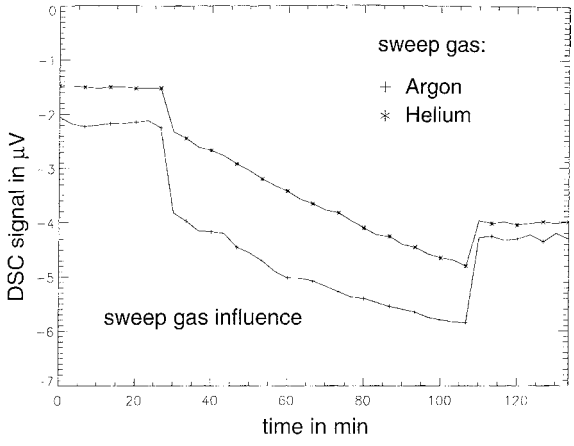

Fig. 1. Influence of sweep gas on the DSC-signal (same conditions of measurements).

system AGEMA THV 900. Fig. 2 shows sample crucibles heated uniformly in a furnace. The evaluation of the thermogram in Fig. 3 illustrates the change of the emissivity of the coated crucibles compared to the Al_2O_3 and platinum crucibles.

The high emissivity ε of Al_2O_3 is responsible for a better heat transfer, at high temperatures, between the sample and reference compared to the platinum crucibles. This leads to a decrease in the temperature difference between the sample side and the reference side of the measuring system ($T_s - T_r$) and, therefore, in the DSC signal. For this reason, investigations were carried out with a platinum crucible as the reference crucible, in spite of the basic requirement of creating conditions which are as identical as possible for sample and reference side. The sample was in an Al_2O_3 crucible for the aforementioned reasons. The basic influence of the emissivity of both crucibles on the DSC signal will be examined by analyzing the heat transport.

2.2. Modelling

For a description of the heat transport processes, a simplified model was chosen, which neglects the contact resistances and suggests the principle of homogeneous temperatures of the measuring system relating to both, the sample (T_s) and the reference (T_r) side. The following essential assumptions are the basis of the model:

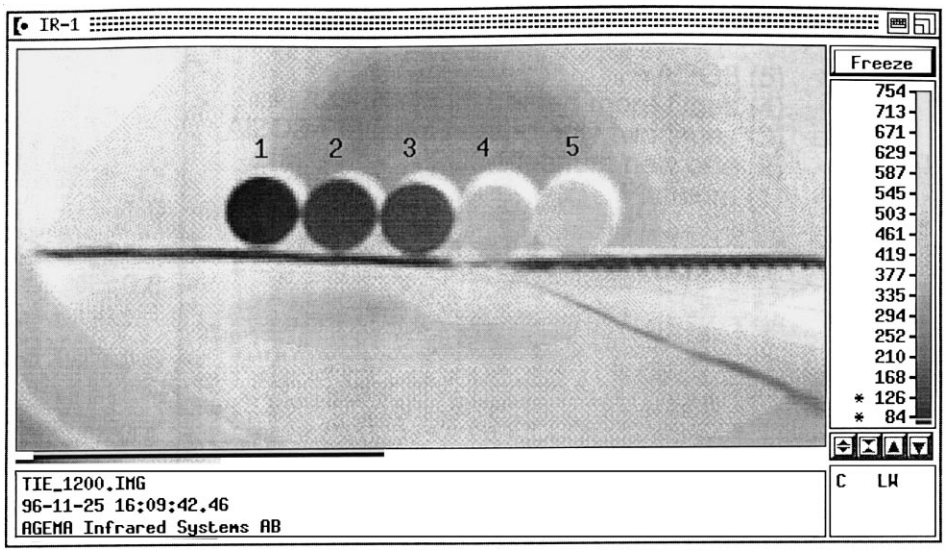

Fig. 2. Infrared thermographic image of different crucibles (for the numbering of crucibles see Fig. 3).

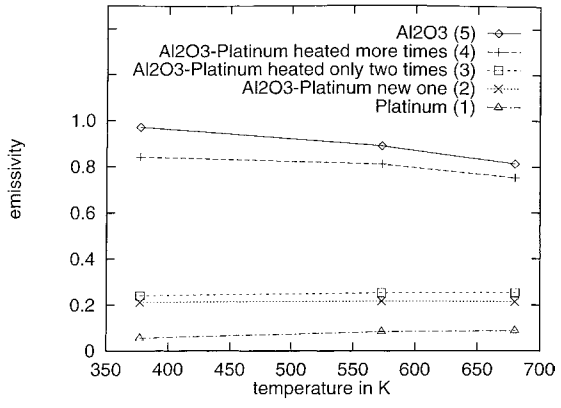

Fig. 3. Experimentally determined emissivity for different crucible surfaces.

- Neglect of the resistances of heat conduction for sample and reference as well as their crucibles (borderline case $Bi \Rightarrow 0$).
- Dominance of radiation heat transfer between furnace and sample crucible ($\dot{Q}_{fs}$) as well as between furnace and reference crucible ($\dot{Q}_{fr}$) at the considered temperature range of T>1000 K.
- Calculation of the heat-transfer coefficient, caused by radiation, from the relationship valid for small differences between furnace temperature T_f and the temperature of measuring system at the sample side T_s:

$$\alpha_{rad} = 4\varepsilon_s\sigma\left(\frac{T_f + T_s}{2}\right)^3 = \varepsilon_s\alpha^*_{rad} \tag{1}$$

- No interactions between sample and reference crucible.
- Quasi-stationary conditions.
- Assumption of a total heat capacity of the empty crucible and its support for both sample ($C_{t,.s}$) and reference ($C_{t,r}$) sides of the transducer.

With these assumptions, the following simplified model equations can be set up:

$$\frac{\dot{Q}_{fs}}{\varepsilon_s} \approx \alpha^*_{rad}A(T_f - T_s) \approx \frac{(mc)_s + C_{t,s}}{\varepsilon_s}\frac{dT_s}{dt} \tag{2}$$

$$\approx \frac{(mc)_s + C_{t,s}}{\varepsilon_s}\left(\frac{dT_r}{dt} + \frac{d\Delta T}{dt}\right) \tag{3}$$

$$\frac{\dot{Q}_{fr}}{\varepsilon_r} \approx \alpha^*_{rad}A(T_f - T_r) \approx \frac{C_{t,r}}{\varepsilon_r}\frac{dT_r}{dt} \tag{4}$$

$$\frac{\dot{Q}_{\mathrm{fs,b}}}{\varepsilon_{\mathrm{s}}} \approx \alpha^{*}_{\mathrm{rad}} A (T_{\mathrm{f}} - T_{\mathrm{s}})_{\mathrm{b}} \approx \frac{C_{\mathrm{t,s}}}{\varepsilon_{\mathrm{s}}} \left[\left(\frac{\mathrm{d}T_{\mathrm{r}}}{\mathrm{d}t} \right)_{\mathrm{b}} + \left(\frac{\mathrm{d}\Delta T}{\mathrm{d}t} \right)_{\mathrm{b}} \right] \tag{5}$$

$$T_{\mathrm{r}} - T_{\mathrm{s}} \approx \frac{1}{\alpha^{*}_{\mathrm{rad}} A} \left[\left(\frac{(mc)_{\mathrm{s}} + C_{\mathrm{t,s}}}{\varepsilon_{\mathrm{s}}} - \frac{C_{\mathrm{t,r}}}{\varepsilon_{\mathrm{r}}} \right) \frac{\mathrm{d}T_{\mathrm{r}}}{\mathrm{d}t} + \frac{(mc)_{\mathrm{s}} + C_{\mathrm{t,s}}}{\varepsilon_{\mathrm{s}}} \frac{\mathrm{d}\Delta T}{\mathrm{d}t} \right] \tag{6}$$

$$(T_{\mathrm{r}} - T_{\mathrm{s}})_{\mathrm{b}} \approx \frac{1}{\alpha^{*}_{\mathrm{rad}} A} \left[\left(\frac{C_{\mathrm{t,s}}}{\varepsilon_{\mathrm{s}}} - \frac{C_{\mathrm{t,r}}}{\varepsilon_{\mathrm{r}}} \right) \left(\frac{\mathrm{d}T_{\mathrm{r}}}{\mathrm{d}t} \right)_{\mathrm{b}} + \frac{C_{\mathrm{t,s}}}{\varepsilon_{\mathrm{s}}} \left(\frac{\mathrm{d}\Delta T}{\mathrm{d}t} \right)_{\mathrm{b}} \right] \tag{7}$$

Eqs. (5) and (7) and the index 'b' refer to the blank run. Assuming quasi-stationary conditions

$$\frac{\mathrm{d}T_{\mathrm{r}}}{\mathrm{d}t} \approx \left(\frac{\mathrm{d}T_{\mathrm{r}}}{\mathrm{d}t} \right)_{\mathrm{b}} \approx \frac{\mathrm{d}T_{\mathrm{f}}}{\mathrm{d}t} \tag{8}$$

and also $\mathrm{d}\Delta T \ll \mathrm{d}T_{\mathrm{r}}$, the signal difference between sample run and blank run is given by the equation

$$(T_{\mathrm{r}} - T_{\mathrm{s}}) - (T_{\mathrm{r}} - T_{\mathrm{s}})_{\mathrm{b}} \approx \frac{1}{\alpha^{*}_{\mathrm{rad}} A} \frac{(mc)_{\mathrm{s}}}{\varepsilon_{\mathrm{s}}} \frac{\mathrm{d}T_{\mathrm{f}}}{\mathrm{d}t} \tag{9}$$

For sufficiently small heating rates, making the quasi-stationary conditions available, the integration of Eq. (9) between two temperature plateaus at T_1 and T_2 provides

$$(mc)_{\mathrm{s}} \int_{T_1}^{T_2} (T_2 - T_1) \approx \varepsilon_{\mathrm{s}} \alpha^{*}_{\mathrm{rad}} A \int_{t_1}^{t_2} [(T_{\mathrm{r}} - T_{\mathrm{s}}) - (T_{\mathrm{r}} - T_{\mathrm{s}})_{\mathrm{b}}] \mathrm{d}t \tag{10}$$

Corresponding to Eq. (10), emissivity of the reference crucible ε_r has no influence on the signal difference of the step-scanning method. But the low emissivity of platinum ($\varepsilon_{\mathrm{Platin}} \approx 0.1 \varepsilon_{\mathrm{Al_2O_3}}$) exerts influence on the level of the single DSC signals (Eqs. (6) and (7)). This effect is equivalent to an increase of heat capacity of the reference side ($C_{\mathrm{t,r}}$). Fig. 4 clearly shows the experimental confirmation of the signal enlargement for a cylindrical platinum sample. The base lines corresponding to both crucible combinations are represented in Fig. 5. Due to the enlarged signals, the signal-to-noise ratio of the individual curves is improved. That facilitates placing the base line for integration of the peaks and reduces the error, see Fig. 6. However, the decisive advantage is the essential decrease in thermal interactions between sample and the reference crucible.

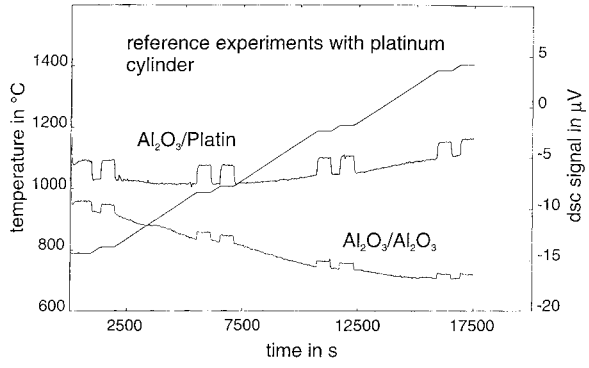

Fig. 4. Experiments with platinum cylinder using different reference crucibles (transducer: DSC; sweep gas: helium; crucibles: Al_2O_3/Pt; sample: platinum; mass: 1.71 g; and heating rate: 3 K/min).

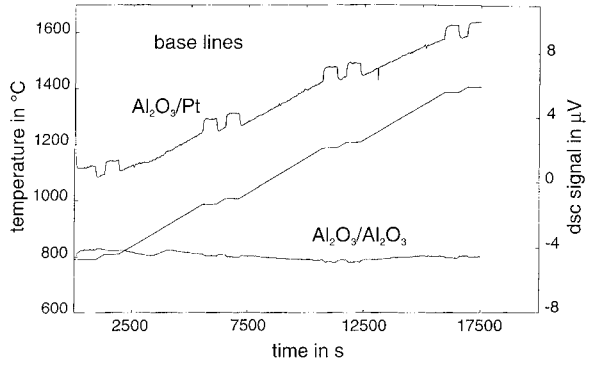

Fig. 5. Base lines for different crucible combinations (transducer: DSC; sweep gas: helium; crucibles: Al_2O_3/Pt; sample: blank; and heating rate: 3 K/min).

2.3. Calibration

Due to the structural transition occurring during the heating up of steels, the continuous-scanning method was used to determine the specific heat. In addition, the step-scanning method was used beyond the transition points. For the continuous method, no calibration is necessary by the evaluation of three runs (sample,

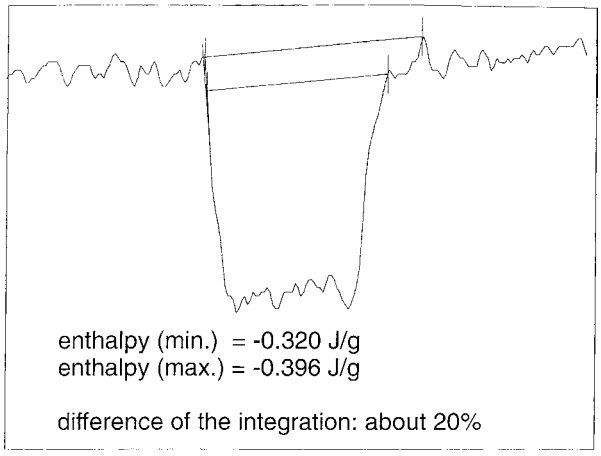

Fig. 6. Possible positions of the base line caused by the signal noise.

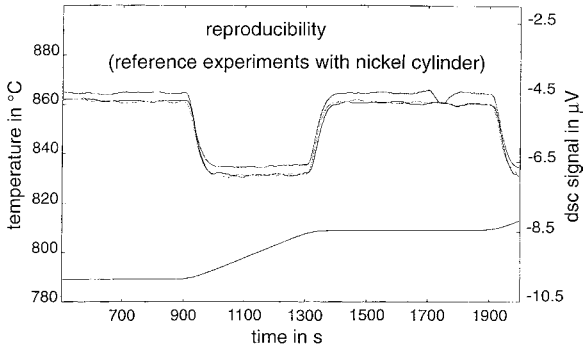

Fig. 7. Reproducibility of DSC-signal (transducer: DSC; sweep gas: helium; crucibles: Al_2O_3/Pt; sample: nickel; mass: 719.1 mg; heating rate: 3 K/min; and temperature interval: 790–810°C).

reference and blank). The choice of a heat capacity of the reference has to be equal, as far as possible, to that of the sample.

This is essential for the reliability of the results. Because of the unknown particular heat capacity of the sample, two or three reference tests may be necessary to approach the heat capacity of the sample.

The influence of using a platinum reference crucible was examined with the step-scanning method. In accordance with the programmed heating up curve, the heat capacities were determined at 1000°, 1200° and 1400°C, respectively. The step between two temperature plateaus was 20 K. For each sample, three measurements were carried out. The good, reproducible results are shown in Fig. 7. In spite of nonidentical curves due to small changes in the signal level, the areas determined by integration are in good agreement.

Nickel, platinum and tungsten cylinders was used as reference materials for the calibration of the signal areas. The cylinders have to be manufactured so as to have a good contact with the bottom of the crucible. One of the signal curves of the calibration runs with platinum cylinder is shown in Fig. 4 (Al_2O_3/Pt crucibles). After repeated steel melting, a new calibration was necessary.

3. Results

3.1. Experimental results

Measurements were carried out for three types of steel. The chemical composition of the steels is illustrated in Table 1. In Fig. 8, the signal curve of S600

Table 1
Chemical composition of steels in %

Steel	C	Si	Mn	P	S	Cr	Ni
S355T	0.17	0.42	1.46	0.032	0.013	0.24	0.05
S600	0.08	0.32	1.38	0.010	0.008	1.44	0.40
X6CrNiMoTi17122	0.03	0.43	1.04	0.025	0.004	16.92	10.63
	Cu	Mo	N	V	Al	Nb	Ti
S355T	0.04	—	0.009	0.01	—	—	—
S600	0.10	0.44	0.009	—	—	0.006	—
X6CrNiMoTi17122	0.16	2.09	—	0.09	0.028	—	0.25

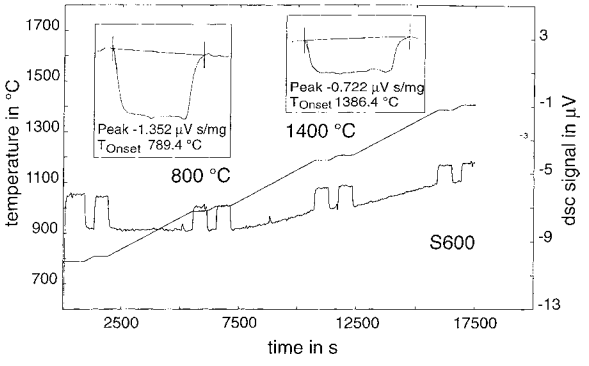

Fig. 8. DSC-curve and signal evaluation for S600 (transducer: DSC; sweep gas: helium; crucibles: Al_2O_3/Pt; sample: S600; mass: 584.1 mg; and heating rate: 3 K/min).

Table 2
Experimentally determined values of specific heat capacity, in J/(gK).

T/ °C	S355T	S600	X6CrNiMoT17122
1000	0.62	0.43	0.44
1200	0.68	0.50	0.53
1400	0.72	0.51	0.74

using the step-scanning method is presented including the evaluation of the areas. The heat capacity was determined, averaging the areas of three tests. The results are shown in Table 2. The relatively high value of the specific heat capacity for steel X6CrNiMoTi17122 at 1400°C may be explained by its proximity to the melting point and by the phase change of particular alloy components. The results for S355T are in a good agreement with the measurements carried out with the continuous-scanning method. These are presented in Fig. 9 in comparison with pure iron. The DSC signal for the melting of S600 and the computed melting enthalpy are shown in Fig. 10. For comparison, the corresponding data of the two other steels are also plotted in the diagram.

Further systematic measurements will be carried out in order to supplement the database *dbs* for the simulation calculations.

3.2. Database

The database *dbs* (Fig. 11) was developed on the basis of thermophysical properties from the available literature to make these properties available for simu-

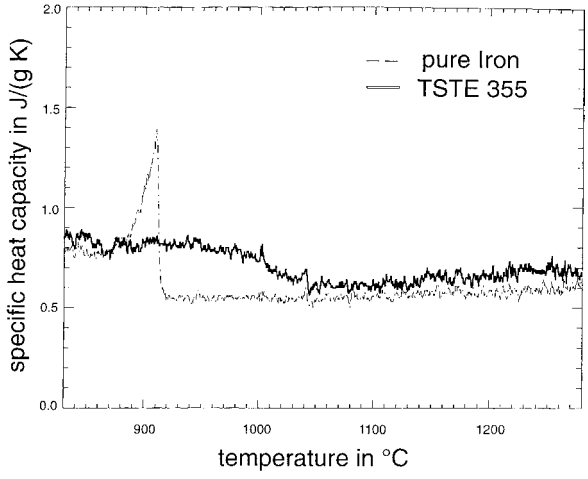

Fig. 9. Specific heat capacity for S355T and pure iron (continuous-scanning method).

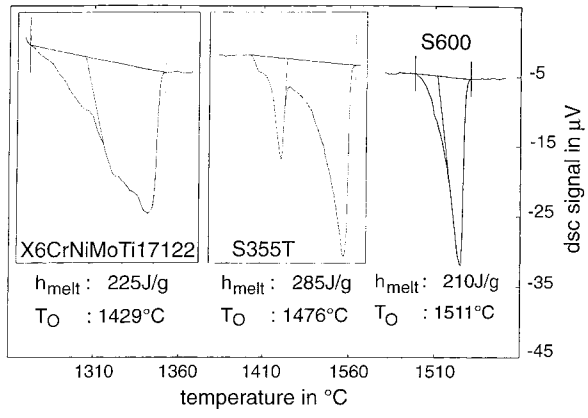

Fig. 10. DSC-signal in the region of melting with evaluation (transducer: DSC; sweep gas: helium; crucibles: Al_2O_3/Al_2O_3; sample: S600; mass: 583.6 mg; and heating rate: 3 K/min).

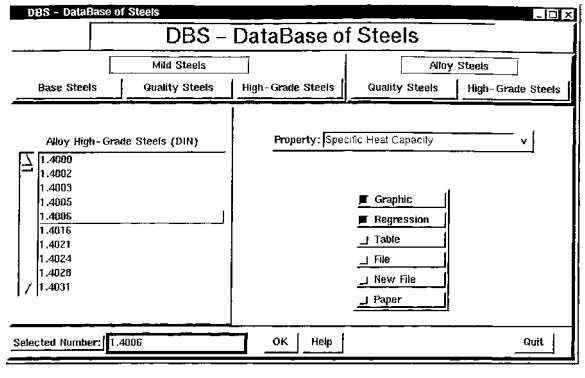

Fig. 11. Main menu on the database *dbs* of steels.

lation computations. The programme was written in the interpreter-language TCL/TK and runs on UNIX and LINUX platforms. All numerical data of a certain steel may be edited and visualized via the main menu. The steels are subdivided in groups according to the European standard EN 10027-2 and can be identified by the steel number. The material property, chosen in the submenu *Property*, can be presented graphically by activating the check button *Graphic* and saved in different graphic formats. The check button *Regression* enables, for example, the polynomial regression up to 10th degree. The activation of the check button *Table* causes a display of the available thermophysical properties. Via the check button *Paper*, a complete document can be made in LaTeX or POSTSCRIPT format. It contains all available information of the selected steel as the nomenclature according to the European Standards, references, alloy composition, regression formulae of the material properties and graphical representations. The numerical data of thermophysical properties and the alloying contribution, taken mainly from the Refs. [6–10], are stored in a defined ASCI format. Hence, the data are available for the programme system *TENAS* [3] too.

The database will be actualized by using results of further experiments to improve the accuracy of the simulation computations.

4. Conclusion

With the database *dbs*, a powerful module for the purpose of thermal simulation calculations is provided. The wide gaps in the availability of thermophysical properties at high temperature require additional experiments, especially for new materials.

The employed thermal analysis system permits the determination of phase change enthalpies and the corresponding temperatures with good accuracy. The determination of specific heat capacities requires a high expenditure, especially due to he calibration. The use of platinum reference crucible improved the signal-to-noise ratio and led to a good reproducibility of the experiments. For a final evaluation of the described method, further experiments and the comparison with measurements made with a high-temperature calorimeter for identical samples are necessary.

A	heat-transfer surface
Bi	Biot number: $Bi=\alpha l_{ch}/\lambda$, l_{ch} – characteristic length
c	specific heat capacity
$C_{t,s}$	total heat capacity of the sample side of the transducer, including crucible
$C_{t,r}$	total heat capacity of the reference side of the transducer, including crucible
m	mass
t	time
T_f	furnace temperature
T_s	temperature of measuring system at the sample side
T_p	phase-change temperature
T_r	temperature of measuring system at the reference side
$\dot{Q}_{fs}$	radiation heat flow rate from furnace to sample side
$\dot{Q}_{fr}$	radiation heat flow rate from furnace to reference side
α_{rad}	heat-transfer coefficient of radiation
α^*_{rad}	modified heat transfer of radiation
ε	emissivity
ε_s	emissivity of sample crucible
ε_r	emissivity of reference crucible
λ_{Ar}	thermal conductivity of argon
λ_{He}	thermal conductivity of helium
σ	Stefan–Boltzmann constant
$\Delta_p h$	phase change enthalpy

Acknowledgements

This research was supported by the Ministry of Education and Cultural Affairs of the Sachsen-Anhalt.

References

[1] D. Weiß, U. Franz, J. Schmidt, A model of temperature distribution and weld pool deformation during arc welding, in: H. Cerjak, H.K.D.H. Bhadeshia (Eds.), Mathematical Modelling of Weld Phenomena II, Institute of Materials, London 1995, pp. 22–39.

[2] D. Weiß, U. Franz, U. Lube, J. Schmidt, Numerical simulation of temperature distribution and seam forming in a narrow gap welding, in: Advanced Computational Methods in Heat Transfer III, Computational Mechanics Publications Southhampton, Boston, 1994, pp. 255–262.

[3] D. Weiß, U. Franz, J. Schmidt, Simulation of weld pool formation during vertical arc welding with emphasis on the influence of groove preparation, TWI, Computer Technology in Welding, 6. Intern. Conference Lanaken, Belgium, 9–12 June 1996, Cambridge, Abington Publ., 1996, paper No. 36, 11 p.
[4] W.F. Hemminger, H.K. Cammenga, Methoden der Thermischen Analyse, Springer-Verlag, Berlin, Heidelberg, 1989.
[5] A. Blažek, Thermal Analysis, Van Nostrand Reinhold Company Ltd, London, 1973.
[6] Y.S. Touloukian, Thermophysical Properties of Matter, Volume 4, Specific Heat, Metallic Elements and Alloys, IFI/PLENUM, New York, Washington, 1970.
[7] Handbuch der Kennwerte von metallischen Werkstoffen, 1. Teil, un- und niedriglegierte Stähle, 2. Teil, hochlegierte Stähle und Nichteisenmetalle, DVS Verlag GmbH Düsseldorf, 1991.
[8] H. Rohloff, A. Zastera, Physikalische Eigenschaften gebräuchlicher Stähle, Verlag Stahleisen GmbH, Düsseldorf, 1996.
[9] F. Richter, Stahleisen-Sonderberichte, Heft 10, Physikalische Eigenschaften von Stählen und ihre Temperaturabhängigkeit, Verlag Stahleisen GmbH, Düsseldorf, 1983.
[10] WUM/WAS (Datenbank), Version 2.0, IMA Materialforschung und Anwendungstechnik GmbH, Dresden, 1994.